

FINAL ADJUSTMENT OF THE MAGNETIC FIELD OF THE LNLS VUV UNDULATOR

G. Tosin, J.F. Citadini, R. Basílio and M. Potye, LNLS, Campinas, Brazil.

Abstract

The first insertion device built at LNLS was an elliptically polarized undulator, designed to cover the vacuum ultraviolet and the soft X-ray spectrum. Its magnetic characterization was done using two techniques: Hall probes, for local field measurements, and rotating coil, operating in a way similar to flip-coil, to determine the integrated multipoles. Final results for the phase errors as well as the procedures used to correct the integrated multipoles are presented.

INTRODUCTION

In the previous Particle Accelerator Conference (EPAC-Scotland, 2006) we presented some reports [1,2] related to the Elliptically Polarized Undulator built at the Brazilian Synchrotron Light Laboratory (LNLS), which has already been installed in the LNLS storage ring [3]. Now we are presenting the final results of the magnetic measurements, and the methods used to refine the undulator magnetic field. Basically, two techniques were used: a rotating coil operating as a flip-coil and the Hall probe mapping.

REFINEMENT OF THE MAGNETIC FIELD

The undulator's magnetic field must cause the minimal disturbance on the stored beam and produce the highest photon flux for any gap or phase. The mechanical design was carefully developed to minimize errors in the magnetic block's position. Also, sorting codes [4] for the magnetic block placement, based on the measured magnetizations, were developed to reduce the magnetic integrated multipoles and optimize the phase error [5]. Sometimes, additional techniques were employed to get information about the non-homogeneity of the block magnetization [6]. All these efforts lead us to an agreement on the order of 10^{-4} T.m between the predicted and the measured linear integrals of the magnetic field.

Even if all the magnets are perfect in geometry and placement and they have the same magnetization, when the phase of the undulator changes, the integrated field also changes. This is an intrinsic magnetic effect of this kind of insertion device and it happens because the permeability of the blocks is different from μ_0 . To illustrate this effect, the undulator was simulated with perfect magnetic blocks and relative permeabilities of 1.06 along the easy axis and 1.17 along the orthogonal axes. Figure 1 shows the linear integration over the horizontal component of the magnetic field (B_x) for five different phase shifts (-25.0, -16.4, 0.0, 16.4 and 25.0 mm) at minimum gap (22 mm) as a function of the transverse position x . It can be seen that for phase 0.0

mm the integrated field is null. Another result is that the vertical field (B_z) is always null, independent of the phase shift and of the transverse position. Although this effect is added to those caused by the magnetic block errors, it is clearly evidenced in the measured data.

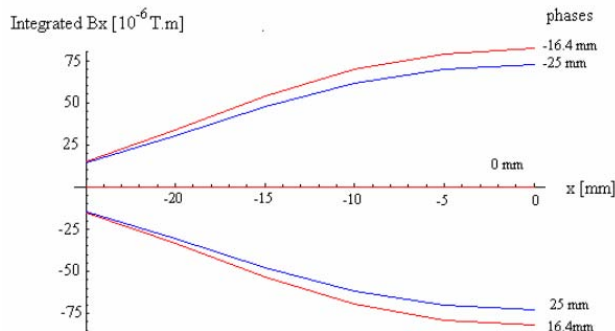


Figure 1. Horizontal linear integrated field simulated for the VUV undulator composed of perfect magnetic blocks. The different phases correspond to linear horizontal, linear vertical and circular light polarizations. This graph is symmetric with respect to the ordinate axis centered in $x = 0$ mm.

Two pairs of air yoke coils (figure 2), one in each extremity of the undulator, were used as correctors (skew multipole correctors) to compensate the variations in the integrated field due to the phase shift. Each pair of coils generates a horizontal integrated field very similar to those shown in figure 1.

The same thin blocks (vertical magnetization) assembled in the undulator termination have been used to correct the normal and skew linear multipoles in the 0.0 mm phase shift (figure 2). Such magnetic arrangement has been denominated "magic pads", a rough version of the magic fingers [7]. When the phase changes, part of the linear integrated field variation comes out because of the permeability effect previously described.

Virtual shims, with displacement freedom of 0.5 mm in both transverse directions, were used to reduce the radiation phase error, while the linear multipoles were always kept within specifications. These multipoles showed low sensitivity to the shimming procedure; therefore, small modifications on the original magic pads arrangement were required. 300 displacements were necessary to reach 3^0 of radiation phase error averaged on phase shifts and gaps, and 560 to reach 2^0 .

Another important feature of this kind of undulator concerns the dynamic multipoles, initially discussed in reference [8]. The expression of the dynamic multipolar expansion (normal or skew) is obtained looking at angular deflections (horizontal or vertical), calculated by a tracking code, as a function of the transverse position x . Such deflections are transformed in linear integrations of

the magnetic field, which will be able to deflect the same angle. Depending on the transverse position of the beam and on the undulator phase-shift and gap, the angular deviation predicted by the linear integration approach can show discrepancies of about 8×10^{-5} T.m when compared to the dynamic calculation.

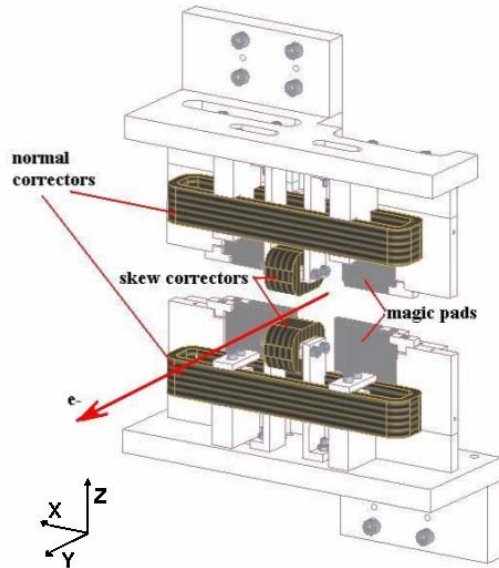


Figure 2. End field structure for multipole corrections. The normal correctors could eventually be used as steering magnets.

This dynamic magnetic effect has its roots in the coupling of the speed (v_z, v_y) with the field components and it would be present even if the magnets were perfect. For vertical field phase (0.0 mm), the coupling is between $v_y B_z$, in regions of transverse B_z gradients; for horizontal field phase (25.0 mm) the effect arises from $v_z B_y$, and for intermediate phases, it is a composition of both couplings. So, it is another intrinsic magnetic effect associated to EPU's (APPLE-II) undulators. Figure 3 shows the dynamic integrated fields for the phases 0.0 and 25.0 mm calculated for the undulator composed of perfect magnets.

Two methods were proposed to keep the dynamic multipoles within multipolar specifications for any phase or gap. The first one was based on the L-shims [8] and the second on couples of small coils. Eight L-shims were applied, two in each cassette at the last periods to minimize their disturbances over the radiation phase error. Figure 4 shows how the L-shims reduce the dynamic multipoles for phase 25.0 mm (horizontal field), which is the worst case. This profile and amplitude are retained for any undulator phase shift.

Another very efficient way to reduce the dynamic multipoles is by placing four small coils at the ends of the undulator (figure 5). However, this solution is much more complex, due to either the coil manufactures or the need of two power supplies, one for each set of diagonally opposite coils. Such configuration allows to correct dynamic multipoles for cassette displacements, happening either in parallel or anti-parallel directions during the

undulator phase shift. The L-shim was the solution adopted, for its easier implementation.

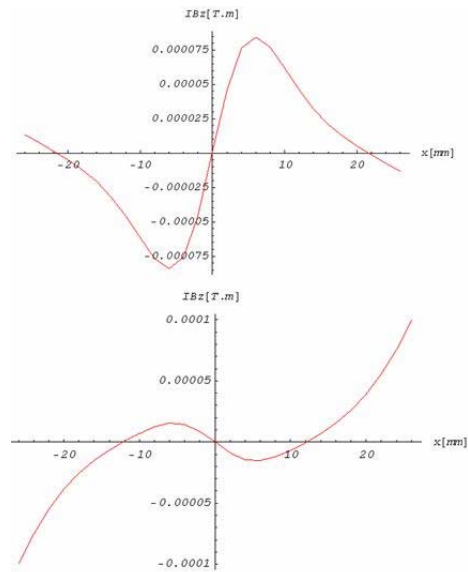


Figure 3. Integrated fields related to horizontal angular deflections, as a function of the transverse position (x). The vertical angular deflection (integration over horizontal component B_x) is very close to zero for any phase shift.

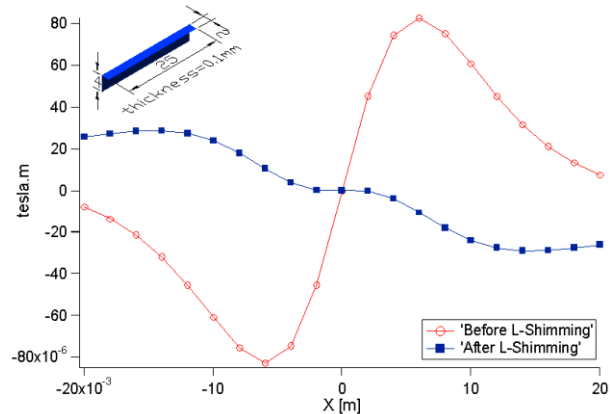


Figure 4. Graph showing the reduction of the dynamic multipoles due to L-shims and their dimensions.

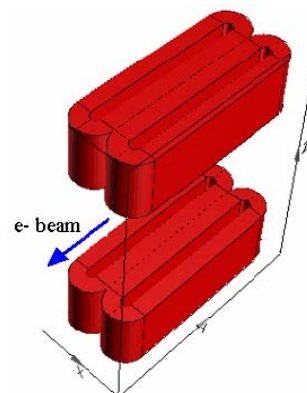


Figure 5. Coils for dynamic multipole reduction. The main dimensions of each coil are 8mmx10mmx35mm.

MEASUREMENTS AND FINAL RESULTS

The set-up for undulator measurements has already been introduced in ref [9]. The rotating coil operated as a flip coil because only the dipolar components of multipolar expansion were taken into account, when the coil was transversally displaced in the horizontal (x) direction. Such dipolar components are calculated from the fast Fourier transformer applied on the induced voltage signal, while in the flip-coil the dipolar integrated field is the average over the coil diameter. Figure 6 shows the linear integrated fields before the L-shims installation and table 1, their respective multipoles.

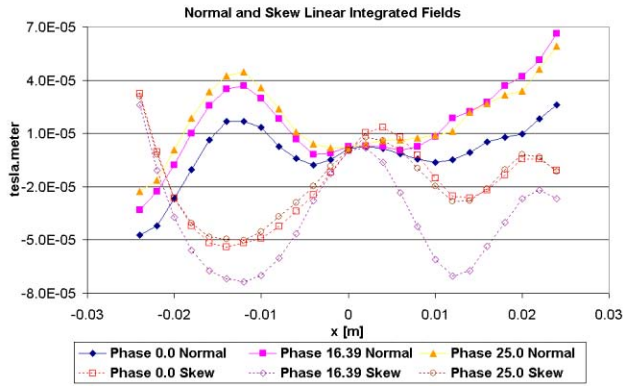


Figure 6. Normal and skew linear integrated fields for some undulator phases at minimum gap.

Table 1. Multipolar coefficients for the curves shown in figure 6.

Normal Multipoles	Phases		
	0.0	16.39	25.0
Dipole [T.m]	-4.0×10^{-6}	-3.0×10^{-6}	-2.0×10^{-7}
Quadrupole [T]	-1.0×10^{-3}	-1.4×10^{-3}	-1.6×10^{-3}
Sextupole [T/m]	1.5×10^{-1}	3.3×10^{-1}	3.4×10^{-1}
Octopole [T/m ²]	$3.4 \times 10^{+0}$	$6.4 \times 10^{+0}$	$5.4 \times 10^{+0}$
Skew Multipoles	0.0	16.39	25.0
Dipole [T.m]	-4.0×10^{-6}	-3.0×10^{-6}	-2.0×10^{-7}
Quadrupole [T]	-1.0×10^{-3}	-1.4×10^{-3}	-1.6×10^{-3}
Sextupole [T/m]	1.5×10^{-1}	3.3×10^{-1}	3.4×10^{-1}
Octopole [T/m ²]	$3.4 \times 10^{+0}$	$6.4 \times 10^{+0}$	$5.4 \times 10^{+0}$

Figure 7 illustrates the dynamic multipoles calculated through the magnetic field map made with Hall probes.

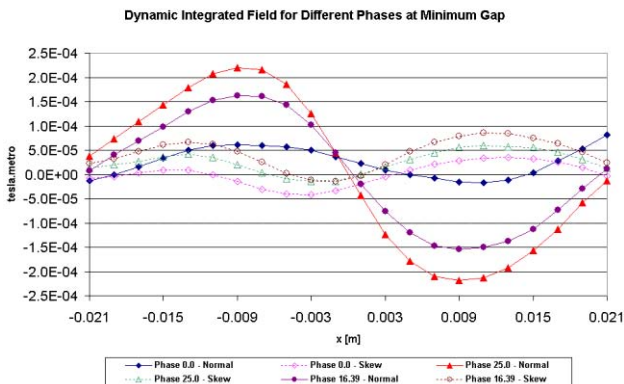


Figure 7. Dynamic integrated field for different phases at minimum gap.

Table 2. Multipolar coefficients based dynamic integrated fields for the graphs presented in figure 7.

Normal Multipoles	Phases		
	0.0	16.39	25.0
Dipole [T.m]	3.6×10^{-5}	1.3×10^{-5}	-1.6×10^{-7}
Quadrupole [T]	-4.5×10^{-3}	2.8×10^{-2}	4.3×10^{-2}
Sextupole [T/m]	-2.3×10^{-1}	-5.7×10^{-2}	1.5×10^{-1}
Octopole [T/m ²]	$9.9 \times 10^{+1}$	$-1.9 \times 10^{+2}$	$-3.1 \times 10^{+2}$
Skew Multipoles	0.0	16.39	25.0
Dipole [T.m]	-3.1×10^{-5}	-1.1×10^{-5}	-7.6×10^{-6}
Quadrupole [T]	-6.7×10^{-3}	-5.4×10^{-3}	-5.1×10^{-3}
Sextupole [T/m]	5.7×10^{-1}	$1.5 \times 10^{+0}$	7.6×10^{-1}
Octopole [T/m ²]	$6.9 \times 10^{+1}$	$6.4 \times 10^{+1}$	$5.8 \times 10^{+1}$

The radiation phase errors, including all gaps and phases of interest, had an average value of 2° with a standard deviation of ±1°.

ACKNOWLEDGE

We thank Johannes Bahrtdt for precious discussion, in special to those topics related to dynamic multipoles.

REFERENCES

- [1] G Tosin et al., “Conceptual Design of an EPU for VUV radiation production at LNLS”, EPAC 2006, Edinburgh, UK, 26-30 June, 2006.
- [2] G Tosin et al., “EPU Assembly based on Subcassettes Magnetic Characterization”, EPAC 2006, Edinburgh, UK, 26-30 June, 2006.
- [3] P.F.Tavares et al., “Commissioning of the LNLS Elliptically Polarizing Undulator”, PAC 2007, Albuquerque, United States, submitted for publication, 2007.
- [4] X. R. Resende and R. M. Dias, “Magnet Sorting Algorithm Applied to the LNLS EPU”, EPAC 2004, Lucerne, Switzerland, 2004.
- [5] R.P. Walker, “Interference effects in undulator and wiggler radiation sources”, Nucl. Instr. and Meth. In Phys. Res. A., v.335, pp.328-337, 1993.
- [6] J. Bahrtdt et al., “Elliptically polarizing insertion devices at BESSY II”, Nucl. Instr. and Meth. In Phys. Res. A., v.467-468, pp.21-29, 2001.
- [7] E. Hoyer et al., “Multiple trim magnets, or “magic fingers”, for insertion device field integral correction, Rev. Sci. Instrum., v. 66, Part 2, pp1901-1903, 1995.
- [8] J. Chavanne et al., “Recent achievements and future prospect of ID activities at ESRF”, EPAC 2000, Vienna, Austria, 2000.
- [9] G Tosin et al., “Development of Insertion Device Magnetic Characterization Systems at LNLS”, EPAC 2006, Edinburgh, Scotland, 2006.